A critical role of DNAM-1 in the development of acute graft-versus-host disease in mice

Tsukasa Nabekura,[1] Kazuko Shibuya,[1] Eri Takenaka,[1] Hirayasu Kai,[1,2] Kai Shibata,[1] Yumi Yamashita,[1] Kyoichi Harada,[1] Satoko Tahara-Hanaoka,[1] Shin-ichiro Honda,[1] and Akira Shibuya[1]

[1] Department of Immunology, Institute of Basic Medical Sciences, Graduate School of Comprehensive Human Sciences, University of Tsukuba, 1-1-1, Tennohdai, Tsukuba, Ibaraki 305-8575, Japan.
[2] Present address: Department of Nephrology, Institute of Clinical Medicine, Graduate School of Comprehensive Human Sciences, University of Tsukuba, 1-1-1, Tennohdai, Tsukuba, Ibaraki 305-8575, Japan.

Address correspondence to Akira Shibuya, MD, PhD (ashibuya@md.tsukuba.ac.jp), or Kazuko Shibuya, MD, PhD (kazukos@md.tsukuba.ac.jp), Phone: (+81) 29-853-3474, Fax: (+81) 29-853-3410

Author contributions: T.N. designed, performed, and analyzed experiments and wrote the paper; E.T., Y.Y., and K.H. assisted T.N. with experiments; H.K. and K. Shibata performed experiments; S.T.-H. and S.H. contributed to data interpretation; and K. Shibuya and A.S. supervised the overall project and wrote the paper.

The authors declare no conflict of interest.

Category: Biological Sciences, Immunology

Abstract

Acute graft-versus-host disease (GVHD) is a life-threatening complication following bone marrow transplantation; however, no effective molecular targeting therapy has been determined. Here, we show that mice that received allogeneic splenocytes deficient in DNAM-1 had significantly milder GVHD and lower mortality than those that received allogeneic wild-type (WT) splenocytes. Donor $CD8^+$ T cells deficient in DNAM-1 showed significantly less proliferation and infiltration of the liver and intestines of recipient mice and produced less interferon (IFN)-γ after coculture with allogeneic splenocytes than WT $CD8^+$ T cells. Mice prophylactically treated with an anti-DNAM-1 antibody showed milder GVHD and lower mortality than those treated with a control antibody. Moreover, treatment with a single administration of the antibody after the overt onset of GVHD ameliorated GVHD and prolonged survival. Finally, we show that the anti-DNAM-1 antibody therapy also ameliorated the overt GVHD in lethally irradiated mice after MHC-matched, minor antigen-mismatched bone marrow transplantation (BMT). These results indicate that DNAM-1 plays an important role in the development of GVHD and is an ideal molecular target for therapeutic approaches to GVHD.

\body

Introduction

Allogeneic bone marrow transplantation (BMT) offers therapy for a variety of hematological malignancies and for both inherited and acquired non-malignant hematological disorders (1, 2). However, the outcome of treatment depends largely on the development of graft-versus-host disease (GVHD), a major and mortal complication of allogeneic bone marrow transplantation (3). Alloreactive donor T lymphocytes that recognize alloantigens in the host are primed by host antigen-presenting cells (APCs), are activated, and mount cellular immune responses against the recipient tissues as “non-self”, damaging host tissues, typically in the liver, gastrointestinal tract, and skin (1, 2, 4). However, the underlying molecular mechanism is incompletely understood. Although immunosuppressants are widely used for prophylaxis and treatment of GVHD, no effective molecular targeting therapy specifically targeting the pathogenesis of GVHD has been determined, contributing to poor prognosis of patients with higher-grade GVHD (5-7).

Although the alloantigen-specific signal mediated by the T-cell receptor is essential for priming of the pathogenic T cells in GVHD development, a costimulatory signal is required for full activation of

the T cells, which leads to the development of exacerbated GVHD (1-3, 8). A strategy to block costimulatory signaling has been established: several blocking monoclonal antibodies (mAbs) and fusion proteins targeting the interaction between costimulatory molecules expressed on T cells and ligands on APCs have been effective in mouse GVHD models (8-12). However, most studies have focused on prophylaxis, not on therapy after the onset of GVHD. Although several blocking approaches have been used in clinical trials, the effects have been inadequate and even deleterious (5-7, 13-16).

The leukocyte adhesion molecule DNAX accessory molecule-1 (DNAM-1, also known as CD226) is a member of the immunoglobulin (Ig) superfamily and is constitutively expressed on most $CD4^+$ T cells, $CD8^+$ T cells, natural killer (NK) cells, monocytes and macrophages, and platelets (17). The poliovirus receptor CD155 and its family member nectin-2 (CD112, also called poliovirus receptor-related family 2) are ligands for DNAM-1 (18, 19). CD155 and CD112 are broadly distributed on hematopoietic, epithelial, and endothelial cells in different amounts in many tissues, as well as in many types of tumors, in human and mouse (20-29). Interactions between DNAM-1 on $CD8^+$ T cells and NK cells and its ligands CD112 and CD155 on target cells augment cell-mediated cytotoxicity (19, 24, 25, 30). Thus, DNAM-1 is involved in a variety of T-lymphocyte functions for the elicitation of appropriate

adaptive immune responses, raising the possibility that it is associated with the severity of several diseases, including cancers, autoimmune diseases, and GVHD.

Here, we explored the role of DNAM-1 in GVHD in a mouse model, and assessed the feasibility of novel prophylactic and therapeutic approaches using blocking antibodies against DNAM-1.

Results

DNAM-1 expression on donor $CD8^+$ T cells, but not recipient cells, is involved in development of acute GVHD

To examine whether DNAM-1 is involved in the pathogenesis of GVHD, we transplanted splenocytes from wild-type (WT) or DNAM-1-deficient (KO) C57BL/6N (B6) (H-2^b) mice into sublethally irradiated B6C3F1 (H-$2^{b/k}$) mice. All the mice that received WT splenocytes died by 50 days after transplantation. In contrast, the mice that received DNAM-1 KO splenocytes lived significantly longer (Fig. 1*A*). Histopathological examination showed that mononuclear cell infiltration and hepatocellular necrosis in the liver and villous atrophy in the small intestine were clearly milder in recipients of DNAM-1-deficient splenocytes (Fig. S1*A*). Liver dysfunction, as determined by serum alanine aminotransferase (ALT) and aspartate aminotransferase (AST) values, and the levels of serum interferon (IFN)-γ were significantly less elevated in the recipients of DNAM-1-deficient splenocytes (Fig. S1*B*, *C*). These results indicate that DNAM-1 expressed on donor cells is involved in the development of GVHD.

To next examine which cell type of donor cells expressing DNAM-1 plays a critical role in the development of GVHD, we prepared both $CD4^+$ and $CD8^+$ T cells-depleted splenocytes (TCD-SP) from

WT B6 mice, and TCD-SP reconstituted with $CD4^+$ (derived from DNAM-1 WT or KO mice) and $CD8^+$ T cells (derived from DNAM-1 WT or KO mice). In contrast to B6C3F1 mice that received TCD-SP alone, recipient mice transplanted with TCD-SP reconstituted with any combinations of $CD4^+$ and $CD8^+$ T cells showed significantly higher levels of ALT and IFN-γ (Fig. S1*D*, *E*). Notably, serum levels of ALT and IFN-γ were higher in mice that received TCD-SP reconstituted with DNAM-1 WT $CD8^+$ T cells than those that received DNAM-1 KO $CD8^+$ T cells-reconstituted TCD-SP, regardless of DNAM-1 expression on donor $CD4^+$ T cells (Fig. S1*D*, *E*). In accordance with these results, recipient mice transplanted with TCD-SP reconstituted with both DNAM-1 WT $CD8^+$ and WT $CD4^+$ T cells showed significantly higher mortality than those that received TCD-SP reconstituted with KO $CD8^+$ T cells and WT $CD4^+$ T cells (upper panel in Fig. 1*B*), while there were no difference in mortality between recipient mice transplanted with TCD-SP reconstituted with DNAM-1 WT $CD8^+$ T cells and WT $CD4^+$ T cells and those transplanted with TCD-SP reconstituted with DNAM-1 WT $CD8^+$ T cells and KO $CD4^+$ T cells (lower panel in Fig. 1*B*). Taken together, these results indicate that DNAM-1 on donor $CD8^+$, rather than $CD4^+$, T cells plays a central role in the development of GVHD.

We further examined whether DNAM-1 expressed on recipient cells is also involved in the

pathogenesis of GVHD. We established a GVHD model, in which splenocytes from WT B6 mice were transplanted into sublethally irradiated WT or DNAM-1 KO CBF1 (H-$2^{b/d}$) mice. A half of mice died by 20 days after transplantation in both recipient groups and there were no significant difference in survival rates between two groups (Fig. 1*C*), suggesting that DNAM-1 expression on recipient cells is not involved in development of acute GVHD.

Anti-DNAM-1 mAb suppresses development of acute GVHD

To examine whether prophylactic treatment with an anti-DNAM-1 neutralizing mAb, TX42 (Fig. S2*A*), suppressed the development of acute GVHD, we injected WT mice with TX42 or control antibody every other day from day -1 until day 17 after transplantation. Although most mice injected with control antibody died within 3 months after transplantation, the mice injected with anti-DNAM-1 mAb lived significantly longer (Fig. 2*A*). Moreover, TX42 dramatically ameliorated injury to the liver and small intestine, compared with control antibody, on day 25 after splenocyte transfer (Fig. 2*B*). In accordance with the histopathological analysis, TX42 prevented the elevation of serum ALT, AST, and IFN-γ (Fig. S3*A*, *B*). These results are similar to those in the recipients of the DNAM-1 KO splenocytes, suggesting

that blockade of DNAM-1 signaling by using a neutralizing mAb *in vivo* prophylactically suppressed the development of acute GVHD.

Anti-DNAM-1 mAb suppresses donor $CD8^+$ T cell proliferation in recipient mice

To explore the role of DNAM-1 on donor cells in the pathogenesis of GVHD, we first used flow cytometry to examine the number of donor $CD4^+$ T cells ($H\text{-}2K^{k\text{-}}CD4^+$) and $CD8^+$ T cells ($H\text{-}2K^{k\text{-}}CD8^+$) in the peripheral blood during the progression of acute GVHD (Fig. S4*A*). Although the numbers of donor $CD4^+$ T cells from DNAM-1 WT and KO mice in the peripheral blood of recipient mice were comparable (left panel in Fig. S4*B*), $CD8^+$ T cells derived from DNAM-1 KO mice were present in significantly lower numbers than those from DNAM-1 WT mice on day 21 after transplantation (right panel in Fig. S4*B*). Similar results were also observed in mice that received TX42 when compared with control antibody (Fig. S4*C*). Moreover, although the frequencies of total donor-derived hematopoietic cells in the liver and small intestine, the major target organs of alloreactive $CD8^+$ T cells in GVHD, was comparable between two groups that received DNAM-1 WT or KO splenocytes (Fig. S4*D*), the populations of donor $CD8^+$ T cells infiltrating into these organs of recipients of DNAM-1 KO

splenocytes were significantly smaller than those in recipients of WT splenocytes (Fig. 3*A*). These results indicate that blocking DNAM-1 signaling limits the proliferation of donor $CD8^+$ T cells *in vivo*. Most donor $CD8^+$ T cells as well as $CD4^+$ T cells from DNAM-1 WT and KO mice differentiated into $CD44^{high}CD62L^{low}$ effector T cells at day 21 after transplantation (Fig. S5), suggesting that there were fewer effector $CD8^+$ T cells in proportion to the total $CD8^+$ T cells in recipients of DNAM-1 KO vs. WT splenocytes or in mice treated with TX42. Taken together with the results shown in Figure 1-3, these results suggest that DNAM-1 on donor $CD8^+$ T cells plays an important role in cell proliferation and infiltration in the liver and small intestine, and is thus involved in the development of acute GVHD.

DNAM-1 costimulation promotes proliferation of and IFN-γ production by alloreactive $CD8^+$ T cells

DNAM-1 mediates a costimulatory signal in cytotoxic T cells and promotes cytotoxicity against target cells expressing DNAM-1 ligands (30, 31). To examine whether DNAM-1 is also involved in the costimulatory effect on proliferation of donor $CD8^+$ T cells after priming *in vivo*, we transplanted CFSE-labeled splenocytes T cells from B6 mice into sublethally irradiated B6C3F1 or B6 mice. In contrast to

$CD8^+$ T cells transplanted into syngeneic mice, most DNAM-1 WT $CD8^+$ T cells transplanted into allogeneic mice had divided at 3 days after transplantation (Fig. S6*A*), suggesting that the cell division resulted from alloantigen recognition. However, fewer DNAM-1 KO $CD8^+$ T cells transplanted into allogeneic mice divided than did WT $CD8^+$ T cells (Fig. S6*A*), indicating that DNAM-1 mediates a costimulatory signal for proliferation in $CD8^+$ T cells *in vivo*. *In vivo* injection with TX42 mAb on day -1 and day 1 after transplantation suppressed cell division of donor $CD8^+$ T cells (Fig. S6*B*). To verify these results *in vitro*, we stimulated CFSE-labeled resting $CD8^+$ T cells from DNAM-1 WT or KO mice with the anti-CD3 mAb plus an anti-DNAM-1 or control Ig. DNAM-1 signaling enhanced the proliferation of resting $CD8^+$ T cells only when $CD8^+$ T cells were simultaneously stimulated with anti-CD3 mAb (Fig. S6*C*, *D*). We also performed the same proliferation assay using donor-derived effector $CD8^+$ T cells sorted from recipient B6C3F1 mice that had been infused with donor B6 splenocytes. As in the resting $CD8^+$ T cells, the proliferation of effector $CD8^+$ T cells was augmented by DNAM-1 costimulation (Fig. S6*E*). The costimulatory effect of DNAM-1 on proliferation was also observed in cocultures of resting or effector $CD8^+$ T cells with allogeneic stimulators such as whole splenocytes (Fig. 3*B*) and either $CD11c^+$ or $CD11c^-$ cells purified from the spleen (Fig. S6*F*). Addition of a neutralizing

anti-CD155 mAb (TX56) in the assay significantly suppressed the alloantigen-specific $CD8^+$ T cell proliferation (Fig. S6*G*), suggesting that CD155 expression on the spelnocytes was involved in DNAM-1-mediated costimulation in $CD8^+$ T cells. Similar to the costimulatory function of DNAM-1 in the proliferation of $CD8^+$ T cells, DNAM-1 also mediated a costimulatory signal for IFN-γ production by resting and effector $CD8^+$ T cells (Fig. S6*H*, *I*). These results demonstrate that DNAM-1 costimulation of alloreactive $CD8^+$ T cells promotes the activation and proliferation of and IFN-γ production by alloreactive $CD8^+$ T cells.

Anti-DNAM-1 mAb suppresses the upregulation of DNAM-1 expression on donor $CD4^+$ and $CD8^+$ T cells in recipient mice

To further investigate the role of DNAM-1 in the pathogenesis of GVHD, we analyzed its expression on donor T cells in recipient mice. B6C3F1 recipient mice received CFSE-labeled splenocytes from WT B6 mice, and the expression of DNAM-1 on donor $CD8^+$ T cells was analyzed by flow cytometry 3 days after transplantation. The mean fluorescence intensity of DNAM-1 on proliferating donor $CD8^+$ T cells was significantly higher than that on non-dividing $CD8^+$ T cells in recipient mice (Fig. 4*A*). To examine

whether the upregulation of DNAM-1 expression on $CD8^+$ T cells was induced by alloantigen recognition, B6 or B6C3F1 recipient mice were transplanted with CFSE-labeled splenocytes from WT B6 mice. Three days after transplantation, DNAM-1 expression on donor $CD8^+$ T cells in the spleen of allogeneic recipient mice was significantly higher than that in syngeneic recipients (Fig. 4*B*). *In vitro* stimulation of $CD8^+$ T cells with an anti-CD3 mAb for 3 days also upregulated DNAM-1 expression (Fig. 4*C*). These results suggest that DNAM-1 expression on alloreactive T cells was upregulated during proliferation in recipient mice. Of note, DNAM-1 on these donor T cells in recipient mice treated with TX42 was significantly less detected by TX42 mAb than in mice treated with control antibody on days 7 to 21 (Fig. S2*C*), probably owing to masking of DNAM-1 by injected TX42 *in vivo* (Fig. S2*B*). Since TX42 mAb is a neutralizing antibody, the masked DNAM-1 on $CD8^+$ cells is not functional. Taken together, these results suggest that development of acute GVHD is associated with upregulated expression of DNAM-1 on donor T cells and anti-DNAM-1 mAb TX42 suppresses DNAM-1 function *in vivo*.

DNAM-1 ligand expression in target organs in acute GVHD

We next examined the expression of DNAM-1 ligands *Cd112* and *Cd155* in target organs in acute GVHD. *Cd112* was expressed predominantly in the liver, large and small intestines, and kidney (Fig. S7). Although *Cd155* was expressed at the highest levels in the heart and kidney, the liver and large and small intestines also expressed a significant amount of *Cd155* (Fig. S7). These results suggest that upregulation of DNAM-1 on alloreactive $CD8^+$ T cells and constitutively high expression of the ligands, particularly CD112, in the liver and intestines are important in the pathogenesis of GVHD. Indeed, the levels of functional DNAM-1 expression detected by TX42 mAb on donor $CD8^+$ T cells were significantly correlated with ALT values (Fig. 4*D*), suggesting that DNAM-1 expression on $CD8^+$ T cells plays a critical role in the exacerbation of GVHD.

Therapeutic treatment with a single administration of anti-DNAM-1 mAb ameliorates GVHD

We next investigated whether treatment with DNAM-1 had a therapeutic effect on overt GVHD. Anti-DNAM-1 mAb TX42 or control Ig was injected i.p. every week into recipient mice from day 14, when GVHD had become overt, to day 77. The mice treated with TX42 mAb showed significantly lower mortality, a dramatic improvement of liver dysfunction (as determined by serum ALT and AST values),

and decreased IFN-γ in the sera after treatment (Fig. 5*A* and Fig. S8*A*, *B*). Injection of TX42 mAb significantly decreased functional DNAM-1 on donor-derived $CD8^+$ T cells, as detected by staining with TX42 mAb (Fig. S8*C*). The amount of functional DNAM-1 on $CD8^+$ T cells was associated with the progression of GVHD, because there was a positive and significant correlation between the amount of functional DNAM-1 on donor-derived $CD8^+$ T cells and ALT values (Fig. S8*D*). Furthermore, the numbers of donor-derived $CD8^+$ T cells in the recipients were decreased after treatment with TX42 (Fig. S8*E*). Therefore, the blockade of DNAM-1 signaling by administration of a blocking mAb against DNAM-1 in a therapeutic setting could inhibit the expansion of alloreactive effector $CD8^+$ T cells even after onset of GVHD. To assess the feasibility of the therapeutic approach with anti-DNAM-1 mAb, we examined whether a single, rather than multiple, administration of anti-DNAM-1 mAb was also effective for the therapy of GVHD. The mice treated with TX42 mAb only on day 14 also showed significantly lower mortality and longer survival (Fig. 5*B*).

Treatment with anti-DNAM-1 mAb ameliorates GVHD in lethally irradiated mice after MHC-matched, minor antigen-mismatched BMT

Finally, we investigated the involvement of DNAM-1 in the development of GVHD in a more clinical-relevant GVHD model after minor-mismatched BMT. Bone marrow cells and T cells from B6 mice (H-2^b) were transplanted into lethally irradiated minor-mismatched C3.SW-$H2^b$-Sn/J (C3) mice (H-2^b). Most recipient mice that were treated with control Ig on day 14 died by 35 days after BMT. In contrast, treatment of the recipient mice with a single administration of TX42 mAb on day 14 significantly prolonged the survival (Fig. 5*C*). These results indicate that the administration of a neutralizing mAb against DNAM-1 is highly potential for therapy as well as prophylaxis for GVHD in a clinical-relevant setting.

Discussion

Given that alloreactive $CD8^+$ T cells primed by host APCs presenting alloantigens directly mediate host tissue injuries in GVHD (2, 3), it is important that this study has clarified the role of DNAM-1-mediated costimulation of pathogenic $CD8^+$ T cells in the development of GVHD. Previous works have revealed that DNAM-1 plays several important roles in modulating cellular immunity, including: 1) the enhancement of cytotoxic T lymphocyte (CTL) (including alloantigen-specific CTL)- and NK cell-mediated cytotoxicity against target cells expressing CD155 or CD112 and cytokine secretion such as IFN-γ, and 2) the proliferation and differentiation of naïve $CD4^+$ T cells toward Th1 cells in cooperation with leukocyte function-associated antigen-1 (LFA-1) (17, 19, 30, 32). Previous report demonstrated that DNAM-1 promoted $CD8^+$ T cell proliferation in response to the presentation of superantigens or OVA peptide antigens by non-professional APCs but not dendritic cells (31). In contrast, we demonstrated that non-professional ($CD11c^-$ cells) as well as professional ($CD11c^+$) APCs in the spleen were involved in the costimulatory effect of DNAM-1 in $CD8^+$ T cells. This discrepancy may be explained by the molecular and functional differences between the alloantigens and the OVA peptide antigen or superantigens. Although emerging evidence supports the involvement of DNAM-1 in

pathogenic T cell-mediated immune diseases, as yet the mechanisms responsible have not been identified. Here we have demonstrated that GVHD exacerbation is due to augmentation of the functions of pathogenic $CD8^+$ T cells by DNAM-1 costimulation, in which the signaling promotes the proliferation of alloreactive T cells immediately after priming, as well as the subsequent clonal expansion of the T cells in the effector phase *in vivo* and *in vitro*. In addition, the enhanced production of IFN-γ by $CD8^+$ T cells dependent on DNAM-1 costimulation potentially contributes to the exacerbation, owing to the immunomodulating effect of IFN-γ on Th1-biased promotion of cellular immunity (33). Thus, our results provide definitive evidence of the critical involvement of DNAM-1 in the pathogenesis of GVHD and of the immunological mechanisms of the exacerbation of the disease.

Most conventional molecular targeting strategies using neutralizing mAbs for prophylaxis for GVHD focus on blocking the interaction between receptors expressed on pathogenic T cells and the ligands on APCs, especially dendritic cells, that leads to priming of T cells in the draining lymph nodes in patients with GVHD, e.g., CD28 and CTLA-4-B7, CD40L-CD40, and LFA-1-ICAM (5, 9-12). The expression of the ligands for these costimulatory receptors is restricted to professional APCs or hematopoietic cells. In contrast, we have shown that two DNAM-1 ligands (CD112 and CD155) are

widely distributed not only on hematopoietic cells, but also on nonhematopoietic cells in many tissues in mice, including the liver and intestines, the major target organs of GVHD (20-22, 26-29, 34, 35). Previous reports demonstrated that the liver expresses *Cd155* much more than the other organs in human (20, 35). Remarkably, we demonstrated that DNAM-1 expression was upregulated on $CD8^+$ T cells after priming and was maintained at high levels on effector T cells in recipient mice. Together, these results suggest that DNAM-1 is involved in effector phase as well as priming phase of alloreactive $CD8^+$ T cells that directly attack the target organs expressing DNAM-1 ligands in the host. This may be one of the reasons why the treatment with anti-DNAM-1 antibody is effective in the therapy as well as prophylaxis for GVHD.

Patients that received BMT are at the high risk of infectious diseases and relapse of hematological and nonhematological tumors under long-term immunosuppressive state. Although the role of DNAM-1 in immune response against infectious diseases remains to be elucidated, we previously demonstrated that DNAM-1 plays an important role in tumor immune surveillance (30). Administration of long-term overabundant dose of a neutralizing mAb against DNAM-1 in a clinical application might be deleterious due to the impairment of graft-versus-leukemia/ tumor effect (GVL/ GVT effect) in patients; however,

attenuation of GVHD with concomitant potent GVL/ GVT effect might be achieved by the regulation of dose and timing of administration of a neutralizing mAb against DNAM-1. In fact, we demonstrated that only a single dose of anti-DNAM-1 mAb dramatically ameliorated GVHD. These results encourage us to test clinical trials of this antibody therapy for GVHD in patients.

The feasibility of conventional strategies for blocking costimulatory molecules in most previous work was examined in prophylactic but not therapeutic approaches in mouse GVHD models (9-11, 36, 37). In sharp contrast, our administration of a neutralizing mAb against DNAM-1 after the clear onset of GVHD ameliorated disease by suppressing alloreactive effector $CD8^+$ T cell proliferation, IFN-γ production and, probably, cytotoxicity against recipient tissue cells. This is the first report using a neutralizing mAb against DNAM-1 for the blockade, and it validates the efficacy of this strategy for the amelioration of GVHD in both MHC-mismatched transplantation and MHC-matched, minor antigen-mismatched BMT in mice. Our GVHD model used MHC-mismatched mouse as a donor, which might be clinically irrelevant. However, since BMT from one locus of HLA-mismatched donor is frequently performed in patients at present, an important point in the present study is that DNAM-1 blocking is able to overcome even a high grade GVHD induced by MHC-mismatched transplantation. Nonetheless, further works aimed at the association of DNAM-1 and its ligands with GVHD pathogenesis induced by transplantation with mismatched minor histocompatibility antigens will be also required for the clinical application of DNAM-1-targeting therapy for GVHD.

Materials and Methods

Materials and methods for mice, antibodies, ELISA, assessment of GVHD, infiltrating donor lymphocytes, proliferation assays, and quantitative RT-PCR used here are described in *SI Materials and Methods*.

GVHD model. Recipient B6C3F1 mice were sublethally irradiated with 500 cGy by X-ray (Hitachi Medical Corporation, Tokyo, Japan). Fifty million splenocytes from DNAM-1 WT or KO B6 mice were intravenously infused into each recipient B6C3F1 mouse. For prophylaxis, 100 μg TX42 was injected i.p. into the recipient mice 1 day before transplantation (day -1) and then every other day for 9 additional doses (total 10 times, 1.0 mg per mouse). For therapy, 300 μg TX42 was injected i.p. beginning on day 14 and then every week for 9 additional doses (total 10 times, 3.0 mg per mouse), or 1.0 mg TX42 was injected i.p. once on day 14.

In some experiments, B6C3F1 recipient mice were transplanted with 3.8 x 10^7 T cell-depleted splenocytes (TCD-SP) alone or the same number of TCD-SP plus 7.0 x 10^6 $CD4^+$ T cells (derived from DNAM-1 WT or KO mice) and 5.0 x 10^6 $CD8^+$ T cells (derived from DNAM-1 WT or KO mice) after

sublethal irradiation with 500 cGy by X-ray. TCD-SP were purified from WT B6 mice by negative selection with biotinylated anti-CD4 and CD8 mAbs, followed with Dynabeads MyONE streptavidin (Invitrogen, Carlsbad, CA). TCD-SP contained T cells at less than 3%, as determined by flow cytometry. $CD4^+$ and $CD8^+$ T cells were purified from the spleens of DNAM-1 WT or KO B6 mice by negative selection with biotinylated anti-B220, CD11b, CD11c, Gr-1, and DX5 (CD49b) mAbs and either biotinylated CD8 or CD4 mAbs, followed with Dynabeads MyONE streptavidin. Purities of $CD4^+$ and $CD8^+$ T cells were more than 85%, as determined by flow cytometry.

To examine whether DNAM-1 on recipient cells is involved in development of GVHD, we generated DNAM-1 WT or KO CBF1 mice ($H\text{-}2^{b/d}$) by crossing *Cd226*$^{+/-}$ Balb/c mice with *Cd226*$^{+/-}$ B6 mice. These mice received 1 x 10^7 splenocytes from WT B6 mice after sublethally irradiation (600 cGy).

For a GVHD model after minor-mismatched BMT, recipient C3 mice were lethally irradiated with 900 cGy one day before BMT (day -1), and then 5 x 10^6 bone marrow cells and 4 x 10^6 spleen T cells from B6 mice were intravenously infused into each recipient mouse on day 0.

Statistical analyses. To analyze survival we used Kaplan-Meier estimation with the statistical analysis

system-type log-rank test. The correlation between DNAM-1 expression levels and ALT values was evaluated with Spearman's rank-order correlation coefficient. All other statistical analyses were performed with the two-tailed Mann-Whitney *U*-test. $P < 0.05$ was considered statistically significant.

Acknowledgments

We thank Lewis L. Lanier (University of California, San Francisco) for critical reading of the manuscript and S. Mitsuishi for secretarial assistance. This research was supported in part by grants provided by the Ministry of Education, Science and Culture of Japan and the Program for Promotion of Fundamental Studies in Health Science of the National Institute of Biomedical Innovation (NIBIO).

References

1. Shlomchik WD (2007) Graft-versus-host disease. *Nat Rev Immunol* 7:340-352.
2. Blazar BR, Korngold R, Vallera DA (1997) Recent advances in graft-versus-host disease (GVHD) prevention. *Immunol Rev* 157:79-109.
3. Reddy P, Ferrara JL (2003) Immunobiology of acute graft-versus-host disease. *Blood Rev* 17:187-194.
4. Shlomchik WD, et al. (1999) Prevention of graft versus host disease by inactivation of host antigen-presenting cells. *Science* 285:412-415.
5. Glennie MJ, Johnson PW (2000) Clinical trials of antibody therapy. *Immunol Today* 21:403-410.
6. Goker H, Haznedaroglu IC, Chao NJ (2001) Acute graft-vs-host disease: pathobiology and management. *Exp Hematol* 29:259-277.
7. Zeiser R, Marks R, Bertz H, Finke J (2004) Immunopathogenesis of acute graft-versus-host disease: implications for novel preventive and therapeutic strategies. *Ann Hematol* 83:551-565.
8. Tanaka J, Asaka M, Imamura M (2000) T-cell co-signalling molecules in graft-versus-host disease. *Ann Hematol* 79:283-290.
9. Blazar BR, Taylor PA, Panoskaltsis-Mortari A, Gray GS, Vallera DA (1995) Coblockade of the LFA1:ICAM and CD28/CTLA4:B7 pathways is a highly effective means of preventing acute lethal graft-versus-host disease induced by fully major histocompatibility complex-disparate donor grafts. *Blood* 85:2607-2618.
10. Blazar BR, Taylor PA, Linsley PS, Vallera DA (1994) In vivo blockade of CD28/CTLA4: B7/BB1 interaction with CTLA4-Ig reduces lethal murine graft-versus-host disease across the major histocompatibility complex barrier in mice. *Blood* 83:3815-3825.
11. Saito K, et al. (1998) Involvement of CD40 ligand-CD40 and CTLA4-B7 pathways in murine acute graft-versus-host disease induced by allogeneic T cells lacking CD28. *J Immunol* 160:4225-4231.
12. Wallace PM, et al. (1994) CTLA4Ig treatment ameliorates the lethality of murine graft-versus-host disease across major histocompatibility complex barriers. *Transplantation* 58:602-610.
13. Devetten MP, Vose JM (2004) Graft-versus-host disease: how to translate new insights into new therapeutic strategies. *Biol Blood Marrow Transplant* 10:815-825.
14. Davies JK, et al. (2008) Outcome of alloanergized haploidentical bone marrow transplantation after ex vivo costimulatory blockade: results of 2 phase 1 studies. *Blood* 112:2232-2241.

15. Cavazzana-Calvo M, et al. (1996) A phase II trial of partially incompatible bone marrow transplantation for high-risk acute lymphoblastic leukaemia in children: prevention of graft rejection with anti-LFA-1 and anti-CD2 antibodies. Societe Francaise de Greffe de Moelle Osseuse. *Br J Haematol* 93:131-138.
16. Vuorte J, et al. (1999) Anti-ICAM-1 monoclonal antibody R6.5 (Enlimomab) promotes activation of neutrophils in whole blood. *J Immunol* 162:2353-2357.
17. Shibuya A, et al. (1996) DNAM-1, a novel adhesion molecule involved in the cytolytic function of T lymphocytes. *Immunity* 4:573-581.
18. Bottino C, et al. (2003) Identification of PVR (CD155) and Nectin-2 (CD112) as cell surface ligands for the human DNAM-1 (CD226) activating molecule. *J Exp Med* 198:557-567.
19. Tahara-Hanaoka S, et al. (2004) Functional characterization of DNAM-1 (CD226) interaction with its ligands PVR (CD155) and nectin-2 (PRR-2/CD112). *Int Immunol* 16:533-538.
20. Baury B, et al. (2003) Identification of secreted CD155 isoforms. *Biochem Biophys Res Commun* 309:175-182.
21. Maier MK, et al. (2007) The adhesion receptor CD155 determines the magnitude of humoral immune responses against orally ingested antigens. *Eur J Immunol* 37:2214-2225.
22. Lopez M, et al. (1998) The human poliovirus receptor related 2 protein is a new hematopoietic/endothelial homophilic adhesion molecule. *Blood* 92:4602-4611.
23. Tahara-Hanaoka S, et al. (2006) Tumor rejection by the poliovirus receptor family ligands of the DNAM-1 (CD226) receptor. *Blood* 107:1491-1496.
24. El-Sherbiny YM, et al. (2007) The requirement for DNAM-1, NKG2D, and NKp46 in the natural killer cell-mediated killing of myeloma cells. *Cancer Res* 67:8444-8449.
25. Verhoeven DH, et al. (2008) NK cells recognize and lyse Ewing sarcoma cells through NKG2D and DNAM-1 receptor dependent pathways. *Mol Immunol* 45:3917-3925.
26. Ravens I, Seth S, Forster R, Bernhardt G (2003) Characterization and identification of Tage4 as the murine orthologue of human poliovirus receptor/CD155. *Biochem Biophys Res Commun* 312:1364-1371.
27. Chadeneau C, LeCabellec M, LeMoullac B, Meflah K, Denis MG (1996) Over-expression of a novel member of the immunoglobulin superfamily in Min mouse intestinal adenomas. *Int J Cancer* 68:817-821.
28. Aoki J, et al. (1997) Mouse homolog of poliovirus receptor-related gene 2 product, mPRR2,

mediates homophilic cell aggregation. *Exp Cell Res* 235:374-384.

29. Morrison ME, Racaniello VR (1992) Molecular cloning and expression of a murine homolog of the human poliovirus receptor gene. *J Virol* 66:2807-2813.
30. Iguchi-Manaka A, et al. (2008) Accelerated tumor growth in mice deficient in DNAM-1 receptor. *J Exp Med* 205:2959-2964.
31. Gilfillan S, et al. (2008) DNAM-1 promotes activation of cytotoxic lymphocytes by nonprofessional antigen-presenting cells and tumors. *J Exp Med* 205:2965-2973.
32. Shibuya K, et al. (2003) CD226 (DNAM-1) is involved in lymphocyte function-associated antigen 1 costimulatory signal for naive T cell differentiation and proliferation. *J Exp Med* 198:1829-1839.
33. Fowler DH, Kurasawa K, Smith R, Eckhaus MA, Gress RE (1994) Donor CD4-enriched cells of Th2 cytokine phenotype regulate graft-versus-host disease without impairing allogeneic engraftment in sublethally irradiated mice. *Blood* 84:3540-3549.
34. Pende D, et al. (2006) Expression of the DNAM-1 ligands, Nectin-2 (CD112) and poliovirus receptor (CD155), on dendritic cells: relevance for natural killer-dendritic cell interaction. *Blood* 107:2030-2036.
35. Iwasaki A, et al. (2002) Immunofluorescence analysis of poliovirus receptor expression in Peyer's patches of humans, primates, and CD155 transgenic mice: implications for poliovirus infection. *J Infect Dis* 186:585-592.
36. Blazar BR, et al. (2003) Ligation of OX40 (CD134) regulates graft-versus-host disease (GVHD) and graft rejection in allogeneic bone marrow transplant recipients. *Blood* 101:3741-3748.
37. Taylor PA, et al. (2005) Targeting of inducible costimulator (ICOS) expressed on alloreactive T cells down-regulates graft-versus-host disease (GVHD) and facilitates engraftment of allogeneic bone marrow (BM). *Blood* 105:3372-3380.

Figure Legends

Fig. 1. DNAM-1 expression on donor $CD8^+$ T cells is involved in exacerbation of acute GVHD.

(*A*) After sublethal irradiation, B6C3F1 mice received splenocytes from DNAM-1 wild-type (WT) (*n* = 14) or knockout (KO) B6 (*n* = 16) mice. B6C3F1 mice that received irradiation only are also shown (*n* = 5). Data are representative of two independent experiments. (*B*) After sublethal irradiation, B6C3F1 recipient mice received T cell-depleted splenocytes (TCD-SP) plus $CD8^+$ T cells from DNAM-1 WT or KO B6 mice and $CD4^+$ T cells from DNAM-1 WT or KO B6 mice (*n* = 10 in each group). Data are pooled from two independent experiments. (*C*) After sublethal irradiation, DNAM-1 WT (*n* = 9) or KO (*n* = 18) CBF1 mice received splenocytes from DNAM-1 WT B6 mice. DNAM-1 WT and KO CBF1 mice that received irradiation alone are also shown (*n* = 5 and 7, respectively). The experiments were independently performed four times and pooled data from all the experiments are shown.

Fig. 2. Anti-DNAM-1 mAb suppressed the development of acute GVHD.

(*A*) After sublethal irradiation, B6C3F1 mice received splenocytes from WT B6 mice. The recipient mice were i.p. injected with anti-DNAM-1 (TX42) (*n* = 14) or control antibodies (*n* = 16) every other

day from day -1 until day 17 after transplantation. B6C3F1 mice that received irradiation only are also shown (n = 10). Data were pooled from three independent experiments. (*B*) The liver and small intestine of mice on day 25 after transplantation were stained with H&E and histologically analyzed. The organs of three mice in each group were analyzed and representative data of a mouse in each is shown. Scale bars indicate 100 μm.

Fig. 3. DNAM-1 is involved in donor $CD8^+$ T cell proliferation in recipient mice after transplantation. (*A*) After sublethal irradiation, B6C3F1 mice received splenocytes from DNAM-1 WT or KO B6 mice. The infiltrating cells in the liver and small intestine in recipient mice (n = 3) on day 14 after transplantation were separated, and each donor-derived ($H\text{-}2K^{k-}$) lymphocyte subset was determined by flow cytometry. Data are representative of two independent experiments. (*B*) Resting $CD8^+$ T cells purified from naïve DNAM-1 WT or KO B6 mice (left panel) and donor effector $CD8^+$ T cells purified from B6C3F1 mice that received WT or KO B6 splenocytes (right panel) were labeled with CFSE, cocultured with mitomycin C-treated syngeneic (B6) or allogeneic (B6C3F1) splenocytes for 3 days, and analyzed by flow cytometry. Data are representative from three independent experiments with similar

results. *$P < 0.05$. Error bars show SD.

Fig. 4. DNAM-1 expression on donor T cells was upregulated in recipient mice.

(*A, B*) After sublethal irradiation, B6C3F1 (allogeneic) or B6 (syngeneic) recipient mice received CFSE-labeled splenocytes from WT B6 mice, and $CFSE^+$ donor $CD8^+$ T cells in the spleen were analyzed by flow cytometry for the expression and mean fluorescence intensity (MFI) of DNAM-1 on day 3 after transplantation. (*C*) $CD8^+$ T cells from B6 mice were stimulated with plate-coated anti-CD3 and analyzed for the expression of DNAM-1 on $CD8^+$ T cells by flow cytometry. (*D*) The correlation between DNAM-1 expression on donor $CD8^+$ T cells on day 21 and ALT values on day 28 in recipients injected with control Ig or TX42 was statistically evaluated. Data are representative of three independent experiments with similar results, respectively. ***$P < 0.005$, *$P < 0.05$. Error bars show SD.

Fig. 5. Anti-DNAM-1 mAb ameliorated overt acute GVHD.

(*A, B*) B6C3F1 mice received splenocytes from WT B6 mice after sublethal irradiation. The recipient mice were injected i.p. with 300 μg anti-DNAM-1 (TX42) ($n = 11$) or control antibodies ($n = 11$) every

week from day 14 until day 77 after transplantation (*A*), or 1.0 mg TX42 (*n* = 19) or control antibodies (*n* = 19) once on day 14 (*B*). B6C3F1 mice that received irradiation only are also shown (*n* = 8 or 9). (*C*) C3 mice were transplanted with bone marrow cells and spleen T cells from B6 mice after lethal irradiation. The recipient C3 mice were injected i.p. with 1.0 mg TX42 (*n* = 8) or control antibodies (*n* = 8) once on day 14. Recipient B6 mice that received transplantation with bone marrow cells and T cells after lethal irradiation (Syngeneic BMT) are also shown (*n* = 6). Data are representative of two independent experiments with similar results in (*A*). Data are pooled from two independent experiments in (*B, C*).

Figures

Nabekura et al.

Figure 1

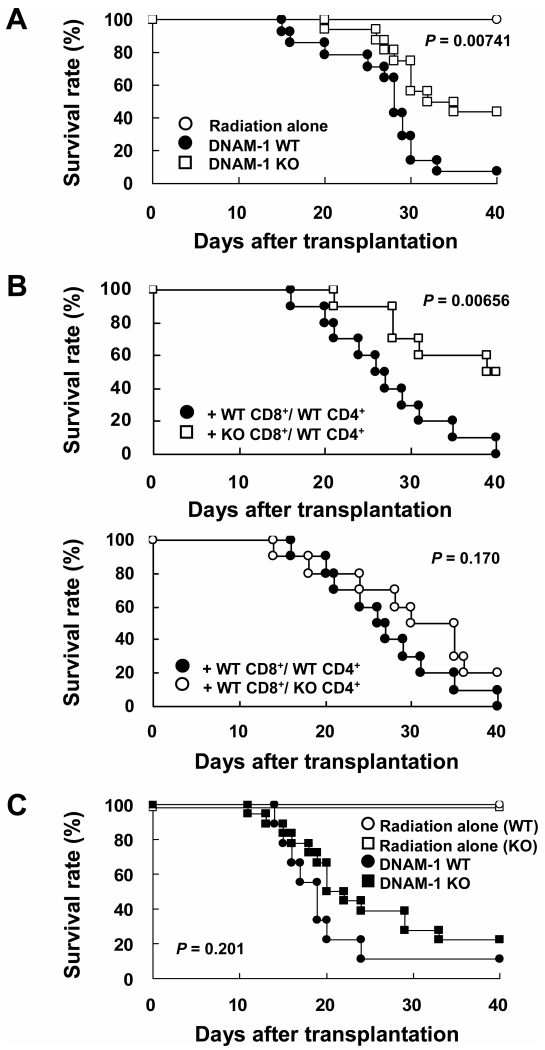

Figure 2

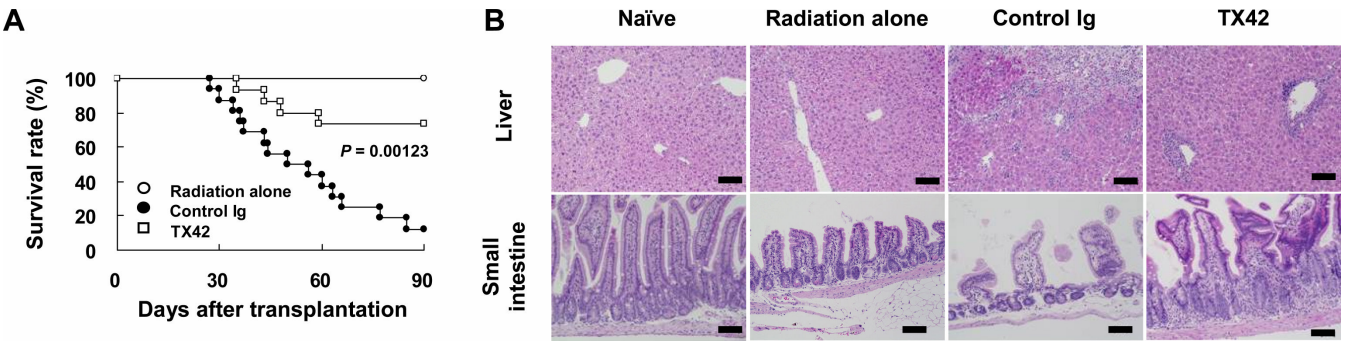
A
Survival rate (%)
100
80
60
40
20
0
0
30
60
90
Days after transplantation
P = 0.00123
Radiation alone
Control Ig
TX42
B
Naïve
Radiation alone
Control Ig
TX42
Liver
Small intestine

Figure 3

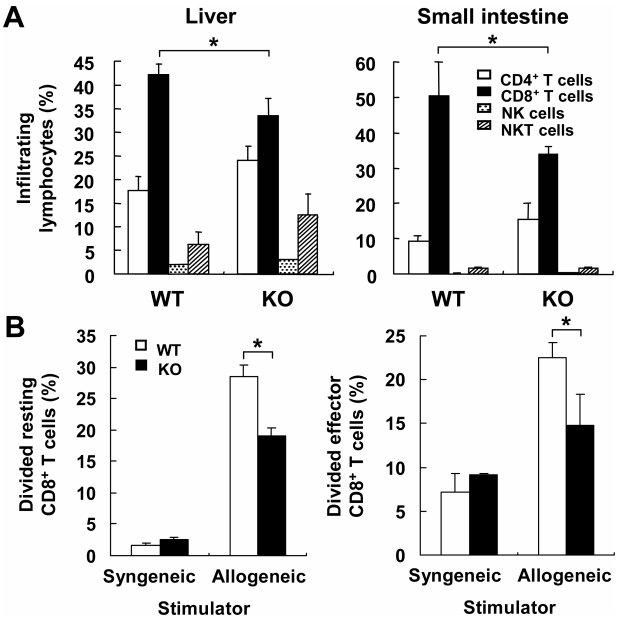
A
Liver
Small intestine
Infiltrating lymphocytes (%)
CD4+ T cells
CD8+ T cells
NK cells
NKT cells
WT
KO
B
Divided resting CD8+ T cells (%)
Divided effector CD8+ T cells (%)
Syngeneic
Allogeneic
Stimulator

Figure 4

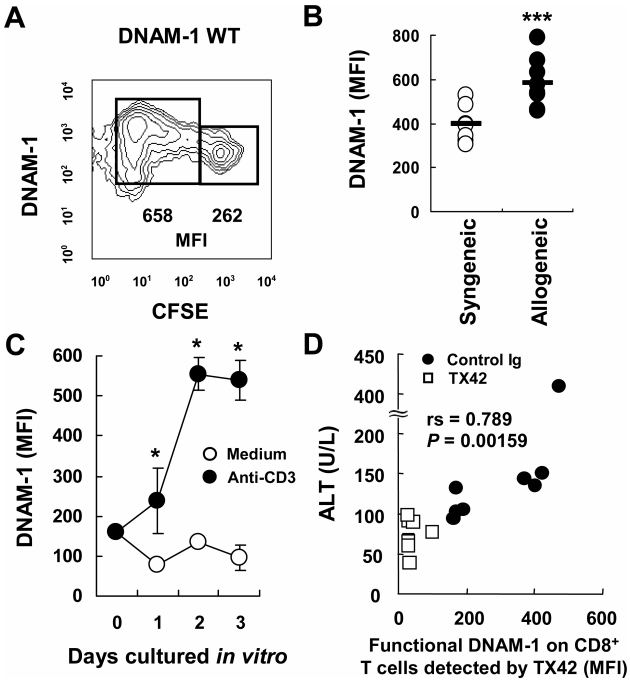
A
DNAM-1 WT
DNAM-1
658
262
MFI
CFSE
B
DNAM-1 (MFI)
***
Syngeneic
Allogeneic
C
DNAM-1 (MFI)
Medium
Anti-CD3
Days cultured *in vitro*
D
ALT (U/L)
Control Ig
TX42
rs = 0.789
P = 0.00159
Functional DNAM-1 on CD8+
T cells detected by TX42 (MFI)

Figure 5

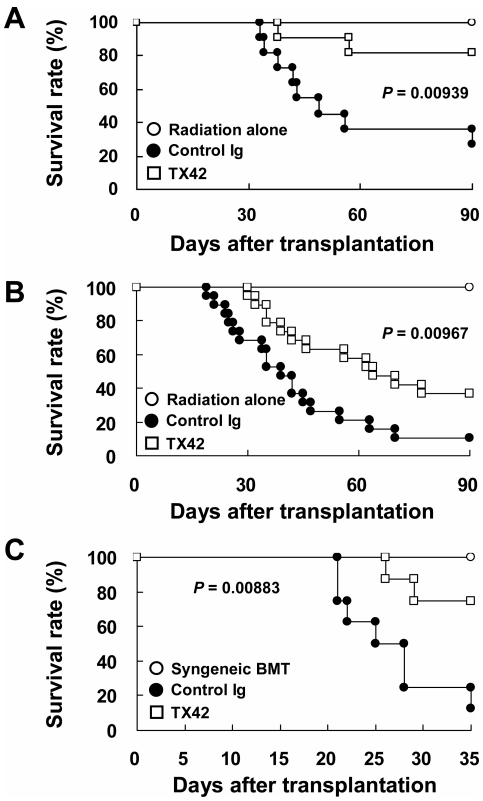
A
Survival rate (%)
100
80
60
40
20
0
P = 0.00939
Radiation alone
Control Ig
TX42
0
30
60
90
Days after transplantation
B
Survival rate (%)
100
80
60
40
20
0
P = 0.00967
Radiation alone
Control Ig
TX42
0
30
60
90
Days after transplantation
C
Survival rate (%)
100
80
60
40
20
0
P = 0.00883
Syngeneic BMT
Control Ig
TX42
0
5
10
15
20
25
30
35
Days after transplantation

Supporting Information

Nabekura et al.

SI Figures and Figure Legends

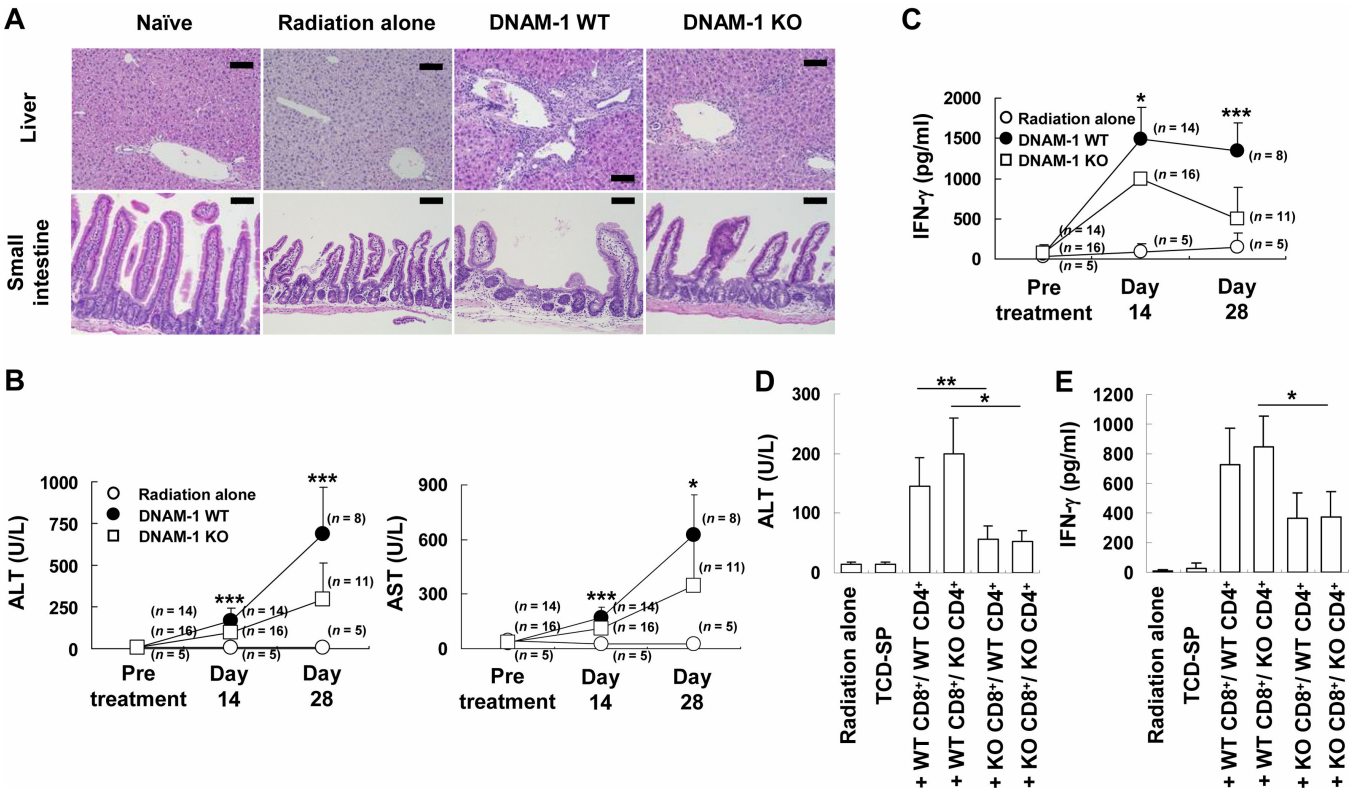

Fig. S1. DNAM-1 expression on donor $CD8^+$ T cells is involved in exacerbation of acute GVHD. (*A-C)* After sublethal irradiation, B6C3F1 mice received splenocytes from DNAM-1 wild-type (WT) (*n* = 14) or knockout (KO) B6 (*n* = 16) mice. B6C3F1 mice that received irradiation only are also shown (*n* = 5). (*A*) The liver and small intestine of mice on day 21 after transplantation were stained with hematoxylin and eosin (H&E) and histologically analyzed. The organs of three mice in each group were analyzed and representative data of a mouse in each is shown. Scale bars indicate 100 μm. (*B*) ALT and AST and (*C*) IFN-γ in the sera of recipient mice was monitored before and after transplantation. Data are representative of two independent experiments. (*D*, *E*) After sublethal irradiation, B6C3F1 recipient mice received T cell-depleted splenocytes (TCD-SP) plus $CD8^+$ T cells from DNAM-1 WT or KO B6 mice and $CD4^+$ T cells from DNAM-1 WT or KO B6 mice (*n* = 5 in each group). B6C3F1 mice that received irradiation alone are shown (*n* = 3) (*D*) ALT and (*E*) IFN-γ in the sera of recipients was measured on day 14 after transplantation. The experiments were performed twice, with the similar

results. One experiment is shown. *$P < 0.05$, **$P < 0.01$, ***$P < 0.005$. Error bars show SD.

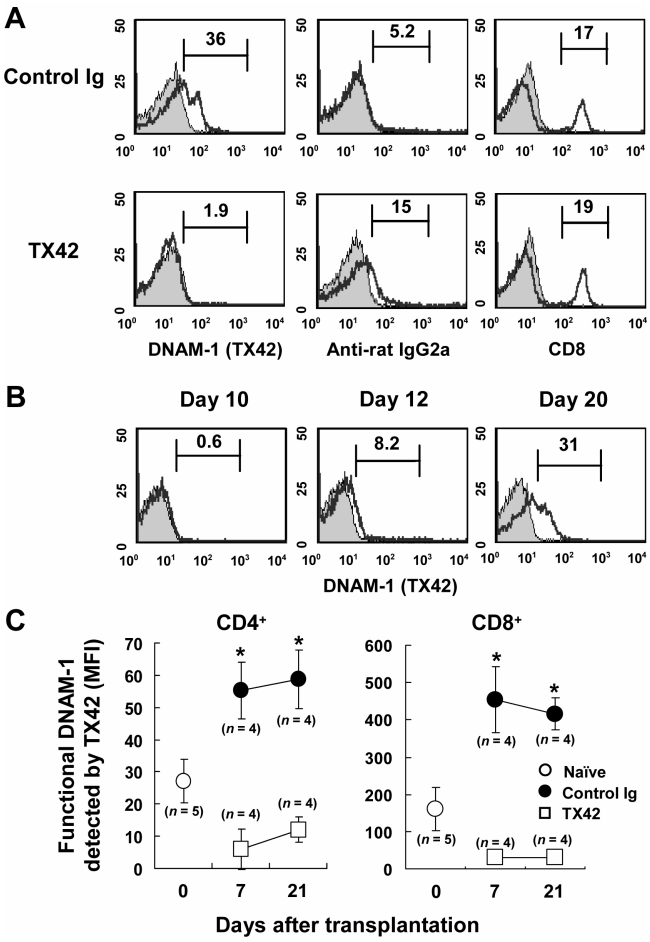

Fig. S2. Characterization of TX42 mAb *in vivo*.

(*A*) Peripheral blood mononuclear cells (PBMC) from B6C3F1 mice that were i.p. injected with 100 μg of control rat IgG2a (upper column) or anti-DNAM-1 mAb, TX42 (rat IgG2a), (lower column) were collected 3 days after the injection, and stained with biotin-conjugated TX42 or isotype-matched control antibody, followed by FITC-conjugated streptavidin. The PBMC were also stained with FITC-conjugated anti-rat IgG2a or anti-CD8 mAbs. Cells were analyzed by flow cytometry. Although $TX42^+$ population was not detected by *in vitro* staining with TX42 in PBMC from the mice on day 3 after TX42 injection, the $DNAM\text{-}1^+$ cell population was detected in mice injected with control rat IgG, suggesting that the pure TX42 mAb continued to bind to DNAM-1 on cell surface *in vivo* for more than 3 days. The populations of $CD8^+$ T cells were comparable between mice that were injected with control IgG and

TX42, indicating that TX42 did not deplete $CD8^+$ T cells. (*B*) PBMC from B6C3F1 mice that were injected i.p. with 100 μg TX42 were collected at the time indicated after the injection, and stained with biotin-conjugated TX42, followed by FITC-conjugated streptavidin. $TX42^+$ population still was not detected on day 12 after TX42 injection, but completely recovered on day 20, indicating that TX42 binding to DNAM-1 on cell surface continues for more than 12 days after TX42 injection. Closed and opened histograms show isotype control and the indicated mAb staining, respectively. Data are representative of three independent experiments with similar results (*A*, *B*). (*C*) After sublethal irradiation, B6C3F1 mice that received DNAM-1 WT splenocytes were i.p. injected with anti-DNAM-1 (TX42) or control antibody every other day from day -1 until day 17 after transplantation. Mean fluorescence intensity (MFI) of DNAM-1 expression on donor $CD4^+$ and $CD8^+$ T cells in the peripheral blood of recipient mice and that on T cells in naïve mice were analyzed by flow cytometry. Data are representative of three independent experiments with similar results. $*P < 0.05$. Error bars show SD.

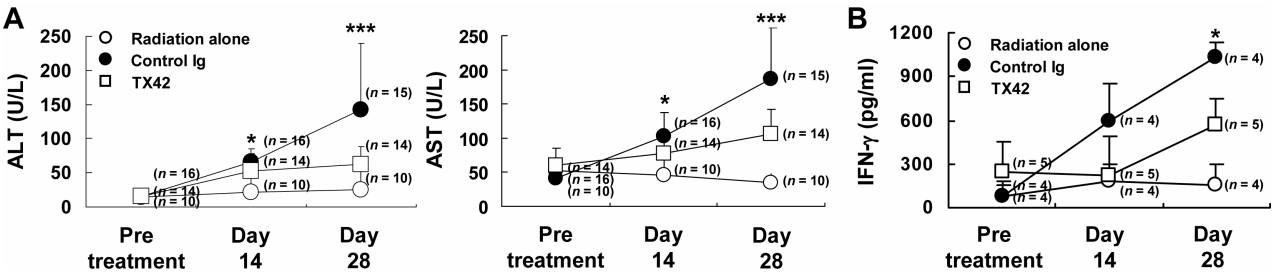

Fig. S3. Anti-DNAM-1 mAb suppressed the development of acute GVHD.

After sublethal irradiation, B6C3F1 mice received splenocytes from WT B6 mice. The recipient mice were i.p. injected with anti-DNAM-1 (TX42) (n = 14) or control antibodies (n = 16) every other day from day -1 until day 17 after transplantation. B6C3F1 mice that received irradiation only are also shown (n = 10). (*A*) ALT and AST and (*B*) IFN-γ in the sera of recipient mice were monitored before and after transplantation. Data are pooled from three independent experiments (*A*, *B*). *$P < 0.05$, ***$P < 0.005$, control Ig vs. TX42. Error bars show SD.

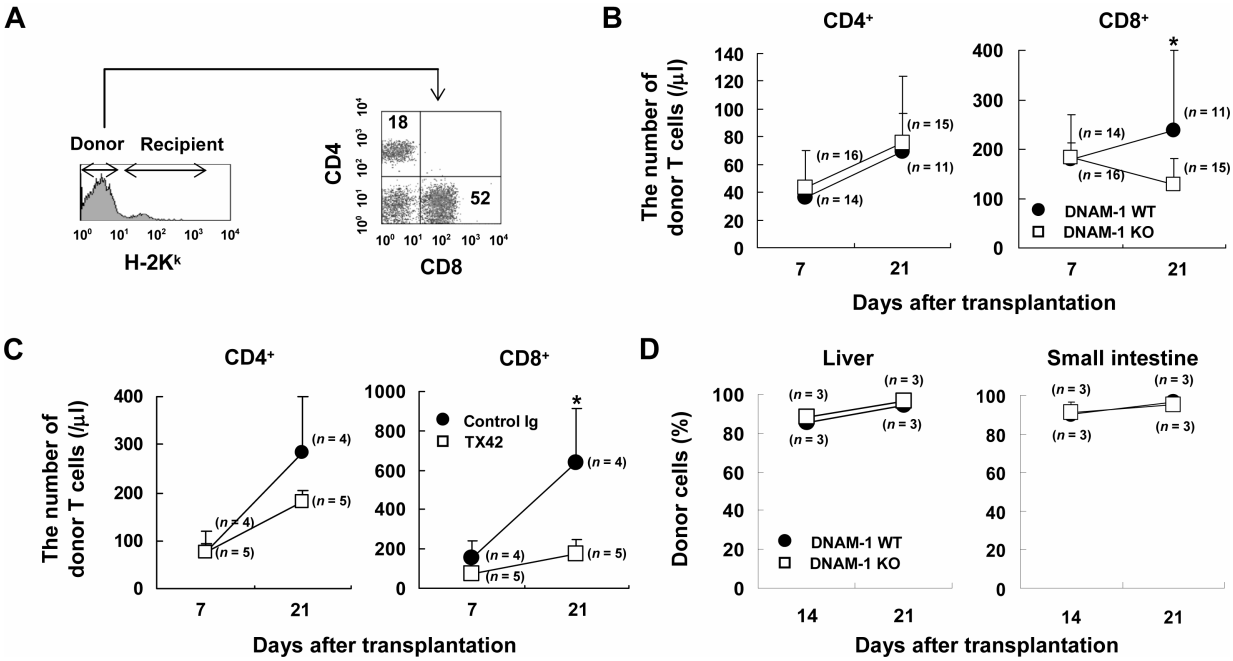

Fig. S4. DNAM-1 is involved in donor $CD8^+$ T cell proliferation in recipient mice.

(*A-D*) After sublethal irradiation, B6C3F1 mice received splenocytes from WT or KO B6 mice. (*C*) Some of the mice that received WT splenocytes were i.p. injected with anti-DNAM-1 (TX42) or control antibodies every other day from day -1 until day 17 after transplantation. (*A*) Peripheral blood cells from the recipient mice were simultaneously stained with FITC-conjugated anti-$H\text{-}2K^k$, PE-Cy5-conjugated anti-CD4, and PE-conjugated anti-CD8 mAbs, and analyzed by flow cytometry. Representative profile of flow cytometry data on day 7 after transplantation is shown. Data are representative of more than five independent experiments. (*B*, *C*) The absolute number of donor $CD4^+$ and $CD8^+$ T cells in recipient peripheral blood was calculated as the number of white blood cells multiplied by the percentage of total donor T cells determined by flow cytometric analysis. Data in (*B*) and (*C*) are representative of two and three independent experiments, respectively. (*D*) On day 14 and 21 after transplantation, the infiltrating donor cells in the liver and small intestine of recipient mice were separated, stained with PerCP-conjugated anti-CD45.2 and FITC-conjugated anti-$H\text{-}2K^k$, and analyzed by flow cytometry. Percentages

of donor cells (H-2K^{k-} gated by CD45.2^{+}) are shown. Experiments were performed twice, with similar results. One experiment is shown. *$P < 0.05$, DNAM-1 WT vs. KO mice (*B*) or control Ig vs. TX42 (*C*). Error bars show SD.

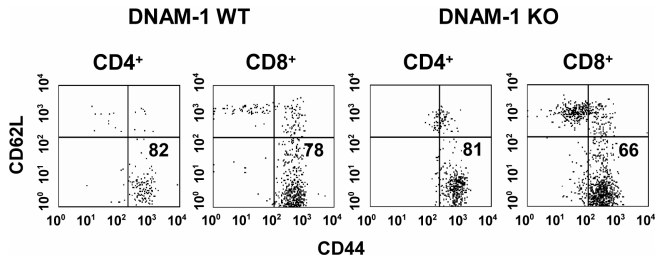

Fig. S5. Differentiation of donor T cells after transplantation.

After sublethal irradiation, B6C3F1 mice received splenocytes from DNAM-1 WT or KO B6 mice, as shown in Fig. 1*A*. On day 21 after transplantation, PBMC were collected and stained with FITC-conjugated anti-H-2K^{k}, APC-conjugated anti-CD44, PE-conjugated anti-CD62L and either PE-Cy5-conjugated anti-CD4 or anti-CD8 mAbs and analyzed by flow cytometry. The profiles on H-2K^{k}-CD4^{+} or H-2K^{k}-CD8^{+} gates are shown. Experiments were performed twice independently (n = 4 in each experiment), with similar results. Data are representative from four mice of one experiment.

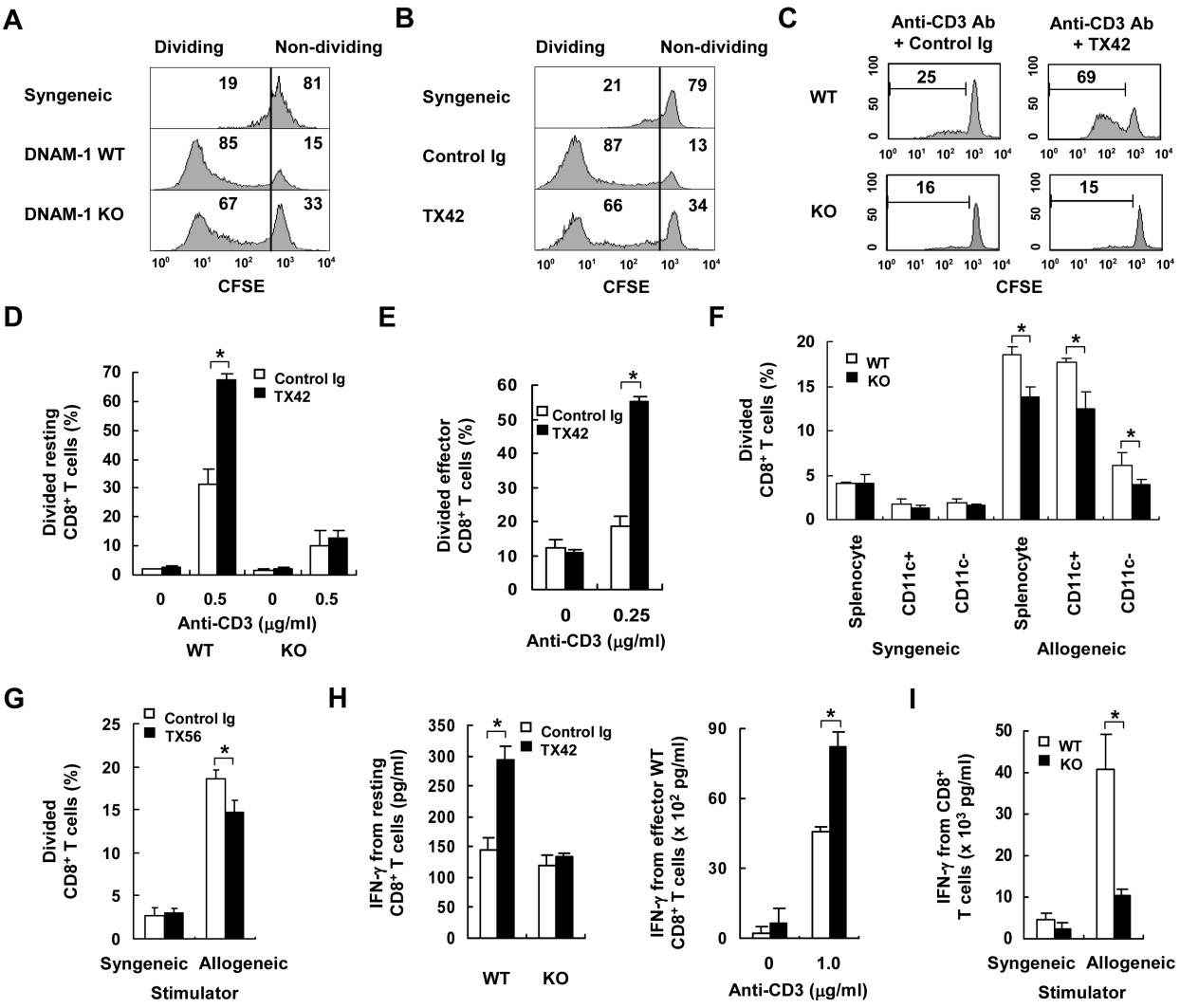

Fig. S6. DNAM-1 mediates a costimulatory signal in $CD8^+$ T cells.

(*A*, *B*) CFSE-labeled splenocytes from DNAM-1 WT ($n = 7$) or KO ($n = 7$) B6 mice were transplanted into sublethally irradiated B6C3F1 mice (A). Recipient B6C3F1 mice were i.p. injected with anti-DNAM-1 (TX42) ($n = 3$) or control antibodies ($n = 3$) on day -1 and day 1 after transplantation of CFSE-labeled splenocytes from WT B6 mice (*B*). CFSE-labeled splenocytes from B6 mice were infused into sublethally irradiated syngeneic mice as a control ($n = 3$). Proliferation of donor $CD8^+$ T cells was analyzed by flow cytometry on day 3 after transplantation. (*C-E*, *H*) Resting $CD8^+$ T cells purified from naïve DNAM-1 WT and KO B6 mice (*C*, *D*), and donor effector $CD8^+$ T cells purified from B6C3F1 mice that received WT B6 splenocytes (*E*) were labeled with CFSE, stimulated or not with plate-coated

anti-CD3 mAb plus anti-DNAM-1 mAb (TX42) or control antibodies for 3 days, and analyzed by flow cytometry (*C*-*E*), and by ELISA for IFN-γ level in the culture supernatants (*H*). Resting $CD8^+$ T cells purified from naïve DNAM-1 WT or KO B6 mice were labeled with CFSE, cocultured with mitomycin C-treated syngeneic (B6) or allogeneic (B6C3F1) splenocytes, dendritic cells ($CD11c^+$), CD11-depleted splenocytes ($CD11c^-$) (*F*), or a neutralizing mAb against CD155 (TX56)- or control antibody-treated splenocytes (*G*) for 3 days, and analyzed by flow cytometry, and by ELISA for IFN-γ level in the culture supernatants (*I*). Data are representative from two or three independent experiments with similar results (*A*-*I*). $*P < 0.05$. Error bars show SD.

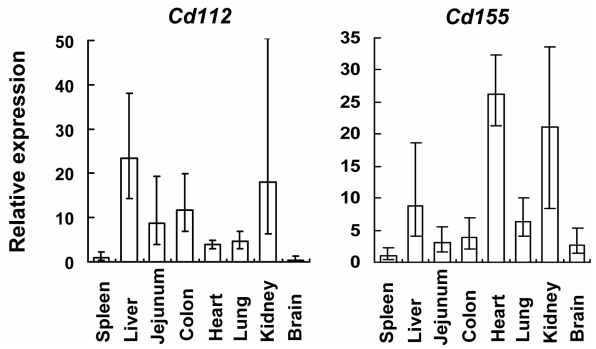

Fig. S7. Expression of the DNAM-1 ligands.

Each organ from B6C3F1 mice was subjected to quantitative RT-PCR for *Cd155* and *Cd112*. Data are means of triplicates. The experiments were performed independently twice, with similar results. Error bars show SD.

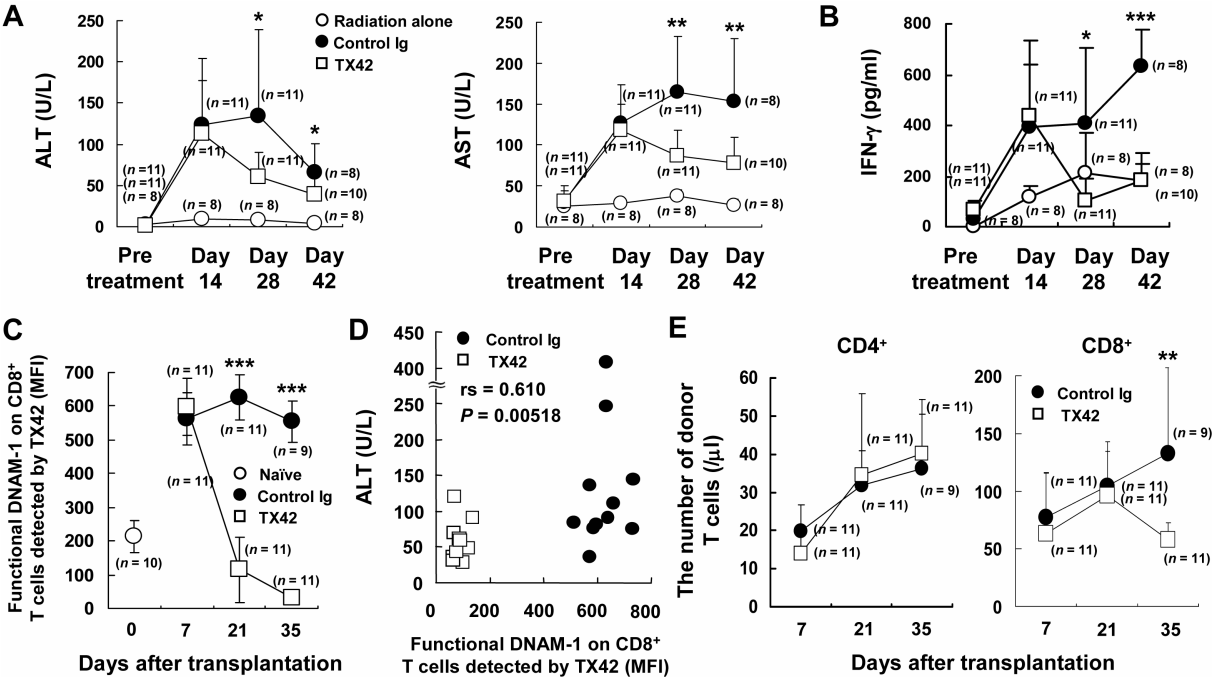

Fig. S8. Anti-DNAM-1 mAb ameliorated overt acute GVHD.

B6C3F1 mice received splenocytes from WT B6 mice after sublethal irradiation. The recipient mice were injected i.p. with anti-DNAM-1 (TX42) (n = 11) or control antibodies (n = 11) every week from day 14 until day 77 after transplantation. B6C3F1 mice that received irradiation only are also shown (n = 8). (*A*, *B*) ALT, AST, and IFN-γ levels in the sera of recipient mice were monitored before and after transplantation. (*C*) MFI of DNAM-1 expression on donor $CD8^+$ T cells in the peripheral blood of the recipient mice was analyzed by flow cytometry. MFI of DNAM-1 expression on $CD8^+$ T cells from naïve B6 mice is also shown. (*D*) The correlation between DNAM-1 expression on donor $CD8^+$ T cells on day 21 and ALT values on day 28 in recipient mice injected with control Ig or TX42 was statistically evaluated. (*E*) PBMC from the recipient mice were simultaneously stained with FITC-conjugated anti-H-$2K^k$, PE-Cy5-conjugated anti-CD4, and PE-conjugated anti-CD8 mAbs, and analyzed by flow cytometry. The absolute number of $CD4^+$ and $CD8^+$ T cells was calculated, as described in Fig. S4*B* and *C*. Data are representative of two independent experiments (*B-E*). *$P < 0.05$, **$P < 0.01$, ***$P < 0.005$,

control Ig vs. TX42. Error bars show SD.